

Energetic bounds on gyrokinetic instabilities.

Part 2. Modes of optimal growth

G.G. Plunk¹ and P. Helander¹

Max Planck Institute for Plasma Physics, 17491 Greifswald, Germany

(Received 9 February 2022; revised 13 May 2022; accepted 16 May 2022)

We introduce modes of instantaneous optimal growth of free energy for the fully electromagnetic gyrokinetic equations. We demonstrate how these ‘optimal modes’ arise naturally from the free energy balance equation, allowing its convenient decomposition, and yielding a simple picture of energy flows. Optimal modes have a number of other favourable features, such as their low dimensionality, efficiency of computation and the fact that their growth rates provide a rigorous and ‘tight’ upper bound on both the nonlinear growth rate of energy, and the linear growth rate of traditional gyrokinetic (normal mode) instabilities. We provide simple closed-form solutions for the optimal growth rates in a number of asymptotic limits, and compare these with our previous bounds.

Key words: plasma instabilities, plasma confinement, plasma nonlinear phenomena

1. Introduction

This is Part 2 in a series, in which we develop a linear and nonlinear stability theory based on gyrokinetic energy balance. Whereas Part 1 emphasizes simple and rigorous upper bounds, this Part 2 shifts focus to tightening these bounds (making them exactly realizable under the right initial conditions), fully generalising their validity (allowing fully electromagnetic fluctuations including non-zero δB_{\parallel}) and introducing the notion of a complete orthogonal set of ‘optimal modes’ associated with these bounds.

Gyrokinetic stability analysis serves as the foundation of turbulence and transport theory for magnetic fusion devices, with linear calculations being the starting point for predicting turbulence intensity and other properties. Such calculations are also the main ingredient of mixing-length estimates (Horton 1999), quasi-linear theory (Staebler, Kinsey & Waltz 2007; Bourdelle *et al.* 2015) and other (indeed, perhaps all) transport models. These linear instabilities are typically understood (with some notable exceptions, e.g. Hatch *et al.* 2016) as ‘normal modes’, i.e. eigenmodes of the linearised gyrokinetic equation, whose time dependence takes the form $\sim \exp(-i\omega t)$, where $\text{Im}[\omega] = \gamma_L$ is the growth rate. When numerically computing gyrokinetic normal modes, it is most common to solve an initial value problem, and terminate the computation only when the solution is found to fit

† Email address for correspondence: gplunk@ipp.mpg.de

the exponential form. This technique yields the mode of largest growth rate for a given wavenumber.

This paper introduces a different kind of gyrokinetic mode, one that realises optimal growth of energy at an instant in time (actually, the idea was proposed first in the gyrokinetic context by Landreman, Plunk & Dorland (2015) but not calculated explicitly there). These modes have been studied extensively in fluid turbulence, where they are called ‘instantaneous optimal perturbations’, and are found as a limit of a more general class of modes that achieve optimal growth of energy over a finite time interval (Farrell & Ioannou 1996).

To illustrate the essential idea of such modes, free from the complications of full gyrokinetics, let us consider a simple schematic equation for a linearised dynamical system with a complex state variable $\psi(t, \ell)$, where t is time and ℓ is a continuous space variable,

$$\frac{\partial \psi}{\partial t} = \mathcal{L}\psi, \quad (1.1)$$

with \mathcal{L} representing some linear operator, whose eigenmodes are precisely the ‘normal modes’ described previously. Defining an inner product (involving, e.g. a suitable average over ℓ), we obtain an ‘energy’ evolution equation for $(\psi, \psi) = \|\psi\|^2$

$$\frac{d\|\psi\|^2}{dt} = (\psi, \mathcal{H}\psi), \quad (1.2)$$

where $\mathcal{H} = \mathcal{L} + \mathcal{L}^\dagger$ is a Hermitian linear operator, with the adjoint operator \mathcal{L}^\dagger defined as that for which $(\psi_1, \mathcal{L}\psi_2) = (\mathcal{L}^\dagger\psi_1, \psi_2)$ holds for arbitrary ψ_1 and ψ_2 in the Hilbert space defined by the inner product.¹ From this we can immediately surmise that the eigenmodes of \mathcal{H} , i.e. ψ_n such that $\mathcal{H}\psi_n = \lambda_n\psi_n$, can be used to characterise the energy growth of the system, as their orthogonality reduces the right-hand side of this equation to the sum of the squares of eigenmode amplitudes, times their eigenvalues. These are precisely the ‘optimal modes’ described previously. Writing $\psi = \sum_n c_n \psi_n$, and taking $\|\psi_n\|^2 = 1$, we have

$$\sum_n \frac{d|c_n|^2}{dt} = \sum_n \lambda_n |c_n|^2. \quad (1.3)$$

Obviously, the eigenmode with the largest positive value achieves optimal growth, i.e. maximises $\|\psi\|^{-2} d\|\psi\|^2/dt$.

Note that ‘instantaneous optimal perturbations’ achieve optimal growth only for an instant. That is, if the system is initialised to be an optimal solution, the observed growth of energy will generally only match the theoretical value initially, and the solution, left undisturbed by nonlinear physics, will evolve over a certain timescale toward a normal mode described previously. Clearly, if this timescale is much longer than the nonlinear decorrelation rate of the turbulence, then the growth of normal modes cannot be expected to be a useful measure, and an alternative measure, such as the optimal rate, may be better. Furthermore, there are cases where turbulence arises when no unstable normal modes exist at all, this being the original motivation for introducing optimal modes. For so-called ‘sub-critical’ turbulence, one needs a measure to characterise the transient linear growth of fluctuations. It is not difficult to see that modes of positive instantaneous optimal growth, one such measure, are *necessary* for sub-critical turbulence to exist

¹We mean ‘Hilbert space’ in the sense of a physicist, i.e. ψ may have dependence proportional to the Dirac delta function when needed (Shankar 1994).

(DelSole 2004). Indeed, from (1.3), the energy of the system can only ever increase if eigenmodes exist with $\lambda_n > 0$.

Even in cases where growth rate of normal modes is found to be a suitable measure of instability, we note that the analysis of optimal modes provides a rigorous upper bound to that growth: if γ is the real part of an eigenvalue of \mathcal{L} in the system above, then $\gamma \leq \max_n \lambda_n/2$.

For gyrokinetics, we can point to several further advantages of optimal modes. The first, as we show, is the drastic reduction in the dimensionality of the problem, as compared with normal mode analysis, for which the kinetic distribution of each particle species requires two velocity variables to be accounted for, in addition to time and space. The complete analysis of optimal modes, in contrast, requires only a few velocity moments to be computed, eliminating the vast majority of the complexity of velocity space. Explicit time evolution, required in initial value computations, is also avoided, and the modes we find are ‘local’ in position space, i.e. the field-line following coordinate becomes merely a parameter of the theory. Furthermore, optimal modes have smooth velocity dependence, making their interpretation more straightforward than that of the singular eigenmodes of linear kinetic plasma theory (e.g. Case–Van Kampen modes), and they form a complete and orthogonal basis for the entire space of gyrokinetic fluctuations. This gives a natural way to decompose energy balance (see (1.3)), and simplifies the analysis of energy flows in the turbulent steady state: the turbulence is excited by unstable modes (with $\lambda_n > 0$) and damped by stable modes (with $\lambda_n < 0$). Optimal mode theory, following directly from energy balance, gives a universal bound on the full ‘zoo’ of gyrokinetic instabilities, in contrast to traditional linear (normal) mode analysis, which requires detailed, separate analysis of different cases. Optimal modes therefore give a unified picture of the space of instabilities, with a much smaller ‘zoo’ than that of the traditional eigenmodes.

As we show, many useful cases of optimal growth can be evaluated with simple closed-form expressions, without the need for numerical computation; when such computation is needed, its cost is trivial. In short, we show that optimal modes can be viewed as a theoretically transparent and computationally efficient alternative (or complement) to normal modes in gyrokinetics.

2. Definitions and gyrokinetic free energy balance

We are interested in finding the solutions that optimise the growth of a certain measure of fluctuation energy. The choice that we have made so far in this series of articles is the gyrokinetic Helmholtz free energy, commonly referred to as simply ‘free energy’. This measure has the advantage of being a ‘nonlinear invariant’, i.e. conserved under nonlinear interactions, and also having a satisfying thermodynamic interpretation: it only diminishes under the action of collisions. These facts are well known and spelled out in Part 1 of this series. We can therefore begin directly with the energy balance equation, which, neglecting collisions, reads

$$\frac{d}{dt} \sum_k H = 2 \sum_k D, \quad (2.1)$$

where the perpendicular wavenumber is $\mathbf{k} = \mathbf{k}_\perp = k_\psi \nabla \psi + k_\alpha \nabla \alpha$, in terms of magnetic coordinates ψ and α such that the equilibrium magnetic field is $\mathbf{B} = \nabla \psi \times \nabla \alpha$. The drive term D is

$$D(\mathbf{k}, t) = \text{Im} \sum_a \left\langle \int g_{a,k} \omega_{*a}^T \bar{\chi}_{a,k}^* d^3v \right\rangle, \quad (2.2)$$

and the free energy is

$$H(\mathbf{k}, t) = \sum_a \left\langle T_a \int \frac{|g_{a,k}|^2}{F_{a0}} d^3v - \frac{n_a e_a^2}{T_a} |\delta\phi_k|^2 \right\rangle + \left\langle \frac{|\delta\mathbf{B}_k|^2}{\mu_0} \right\rangle, \quad (2.3)$$

where $|\delta\mathbf{B}_k|^2 = |k_\perp \delta A_{\parallel k}|^2 + |\delta B_{\parallel k}|^2$, and we define the other notation as follows. The space average is defined as²

$$\langle \dots \rangle = \lim_{L \rightarrow \infty} \int_{-L}^L (\dots) \frac{dl}{B} / \int_{-L}^L \frac{dl}{B}. \quad (2.4)$$

The diamagnetic frequencies are

$$\left. \begin{aligned} \omega_{*a} &= \frac{k_a T_a}{e_a} \frac{d \ln n_a}{d\psi}, \\ \omega_{*a}^T &= \omega_{*a} \left[1 + \eta_a \left(\frac{m_a v^2}{2T_a} - \frac{3}{2} \right) \right]. \end{aligned} \right\} \quad (2.5)$$

The gyro-averaged electromagnetic potential is

$$\bar{\chi}_{ak} = J_0 \left(\frac{k_\perp v_\perp}{\Omega_a} \right) (\delta\phi_k - v_\parallel \delta A_{\parallel k}) + J_1 \left(\frac{k_\perp v_\perp}{\Omega_a} \right) \frac{v_\perp}{k_\perp} \delta B_{\parallel k}, \quad (2.6)$$

and J_0 and J_1 are Bessel functions. Field perturbations are given by

$$\sum_a \frac{n_a e_a^2}{T_a} \delta\phi_k = \sum_a e_a \int g_{a,k} J_{0a} d^3v, \quad (2.7)$$

$$\delta A_{\parallel k} = \frac{\mu_0}{k_\perp^2} \sum_a e_a \int v_\parallel g_{a,k} J_{0a} d^3v, \quad (2.8)$$

$$\delta B_{\parallel k} = -\frac{\mu_0}{k_\perp} \sum_a e_a \int v_\perp g_{a,k} J_{1a} d^3v, \quad (2.9)$$

where we define $J_{na} = J_n(k_\perp v_\perp / \Omega_a)$. Henceforth, we consider a single fixed value of \mathbf{k} and therefore suppress the \mathbf{k} subscripts.

Note that we define the free energy as twice that which appears in some other publications, but this has no significant effect on the analysis, as the 2 drops out of the optimisation problem, upon division by H .

3. Modes of optimal instantaneous growth

To recast (2.1) in the form of (1.2) requires first identifying the state variable(s) and inner product. We take the state to be the set of distributions functions, given by the vector \mathbf{g} with components g_a , and define the inner product of two states \mathbf{g}_1 and \mathbf{g}_2 as

$$(\mathbf{g}_1, \mathbf{g}_2) = \sum_a \left\langle T_a \int \frac{g_{a1}^* g_{a2}}{F_{a0}} d^3v \right\rangle. \quad (3.1)$$

Comparing with (2.3), we note that the free energy H is not the Euclidean norm in these variables (though it is positive-definite in \mathbf{g} for non-zero wavenumber; see

²Our results also hold for a more general definition of the space average, as discussed in Helander & Plunk (2022).

Helander & Plunk 2022). Although it is possible to transform to new state variables, i.e. \tilde{g} such that $H = \|\tilde{g}\|^2$, we find it is more convenient to take another approach at this stage, namely to formulate our problem in variational terms. That is, we extremise the ratio

$$\Lambda = D/H \tag{3.2}$$

over the space of distribution functions g . Note that, as is easily verified, normal modes satisfy $\gamma_L = D/H$, so that we have the bound on so-called linear gyrokinetic instabilities:

$$\gamma_L \leq \max_{g_a} \Lambda. \tag{3.3}$$

Variation of (3.2) leads to the condition

$$\frac{\delta D}{\delta g_a} - \Lambda \frac{\delta H}{\delta g_a} = 0. \tag{3.4}$$

Note that Λ , which according to (2.1) corresponds to *half* the growth rate of free energy, can be interpreted as the Lagrange multiplier whose role is to hold H fixed.

Using (2.2) and (2.3), we can evaluate (3.4) to obtain (see Appendix A)

$$\Lambda \sum_b \mathcal{H}_{ab} g_b = \sum_b \mathcal{D}_{ab} g_b, \tag{3.5}$$

where \mathcal{H} and \mathcal{D} are, respectively, purely real and purely imaginary Hermitian linear operators on the space of distribution functions, given as follows:

$$\mathcal{H}_{ab} g_b = \delta_{a,b} g_b + \frac{F_{a0}}{n_a T_a} \frac{1}{n_b} \int d^3 v' g'_b \left[-\sigma_a \sigma_b \psi_{1a} \psi'_{1b} + \varepsilon_a \varepsilon_b (\psi_{3a} \psi'_{3b} + \psi_{5a} \psi'_{5b}) \right], \tag{3.6}$$

noting that the species label b is not to be confused with the argument of the Bessel functions, and $\delta_{a,b}$ is the discrete delta function. The second operator is given by

$$\begin{aligned} \mathcal{D}_{ab} g_b = & \frac{i}{2} \frac{F_{a0}}{n_a T_a} \frac{1}{n_b} \int d^3 v' g'_b \left[\omega_{*a} (1 - 3\eta_a/2) (\sigma_a \sigma_b \psi_{1a} \psi'_{1b} - \varepsilon_a \varepsilon_b \psi_{3a} \psi'_{3b} - \varepsilon_a \varepsilon_b \psi_{5a} \psi'_{5b}) \right. \\ & - \omega_{*b} (1 - 3\eta_b/2) (\sigma_a \sigma_b \psi_{1a} \psi'_{1b} - \varepsilon_a \varepsilon_b \psi_{3a} \psi'_{3b} - \varepsilon_a \varepsilon_b \psi_{5a} \psi'_{5b}) \\ & + \omega_{*a} \eta_a (\sigma_a \sigma_b \psi_{2a} \psi'_{1b} - \varepsilon_a \varepsilon_b \psi_{4a} \psi'_{3b} - \varepsilon_a \varepsilon_b \psi_{6a} \psi'_{5b}) \\ & \left. - \omega_{*b} \eta_b (\sigma_a \sigma_b \psi_{1a} \psi'_{2b} - \varepsilon_a \varepsilon_b \psi_{3a} \psi'_{4b} - \varepsilon_a \varepsilon_b \psi_{5a} \psi'_{6b}) \right], \end{aligned} \tag{3.7}$$

where primes denote evaluation at v' , and we define

$$\sigma_a = e_a n_a \left(\sum_{a'} \frac{n_{a'} e_{a'}^2}{T_{a'}} \right)^{-1/2}, \tag{3.8}$$

$$\varepsilon_a = e_a n_a \left(\frac{\sqrt{\mu_0} v_{Ta}}{k_{\perp}} \right) = \text{sgn}(e_a) \sqrt{n_a T_a \beta_a / b_a}, \tag{3.9}$$

where $\text{sgn}(e_a) = \pm 1$ gives the sign of e_a , $b_a = k_{\perp}^2 m_a T_a / (e_a^2 B^2)$, the plasma beta of species a is $\beta_a = 2\mu_0 n_a T_a / B^2$, and its thermal velocity is denoted $v_{Ta} = \sqrt{2T_a / m_a}$. We also

introduce velocity-dependent functions that are needed for forming the relevant moments

$$\left. \begin{aligned} \psi_{1a} &= J_{0a}, & \psi_{2a} &= \frac{v^2}{v_{Ta}^2} J_{0a}, & \psi_{3a} &= \frac{v_{\parallel}}{v_{Ta}} J_{0a}, \\ \psi_{4a} &= \frac{v_{\parallel} v^2}{v_{Ta}^3} J_{0a}, & \psi_{5a} &= \frac{v_{\perp}}{v_{Ta}} J_{1a}, & \psi_{6a} &= \frac{v_{\perp} v^2}{v_{Ta}^3} J_{1a}. \end{aligned} \right\} \quad (3.10)$$

3.1. *Moment form of (3.5)*

Equation (3.5) describes an eigenproblem whose solutions form a complete orthogonal basis for the space of distribution functions g_a . This is a large space, but as we show, the non-trivial solution space of (3.5) is actually quite small. There are a number of reasons for this, but the first and most important is that only a small set of velocity moments appear in this equation. We can identify six dimensionless moments for each species, defined as

$$\kappa_{na} = \frac{1}{n_a} \int d^3 v \psi_{na} g_a. \quad (3.11)$$

We further note that, due to the summation over species involved in the computation of the electromagnetic fields and free energy balance, the velocity moments κ_n appear in particular linear combinations. Thus, there is an additional dimensional reduction corresponding to the number of species N_s , i.e. $6N_s \rightarrow 6$. This is achieved with the help of the following barred variables

$$\left. \begin{aligned} \bar{\kappa}_1 &= \sum_a \sigma_a \kappa_{1a}, & \bar{\kappa}_2 &= \sum_a \sigma_a \bar{\omega}_{*a} ((1 - 3\eta_a/2)\kappa_{1a} + \eta_a \kappa_{2a}), \\ \bar{\kappa}_3 &= \sum_a \varepsilon_a \kappa_{3a}, & \bar{\kappa}_4 &= \sum_a \varepsilon_a \bar{\omega}_{*a} ((1 - 3\eta_a/2)\kappa_{3a} + \eta_a \kappa_{4a}), \\ \bar{\kappa}_5 &= \sum_a \varepsilon_a \kappa_{5a}, & \bar{\kappa}_6 &= \sum_a \varepsilon_a \bar{\omega}_{*a} ((1 - 3\eta_a/2)\kappa_{5a} + \eta_a \kappa_{6a}), \end{aligned} \right\} \quad (3.12)$$

where we introduce the normalised frequency $\bar{\omega}_{*a} = \omega_{*a}/\omega_*$, with ω_* an arbitrary reference value. Evaluating the sum over species in (3.5) yields

$$\begin{aligned} & \frac{\Lambda}{\omega_*} \left(g_a + \frac{F_{a0}}{n_a T_a} [-\sigma_a \psi_{1a} \bar{\kappa}_1 + \varepsilon_a (\psi_{3a} \bar{\kappa}_3 + \psi_{5a} \bar{\kappa}_5)] \right) \\ &= \frac{i}{2} \frac{F_{a0}}{n_a T_a} \left[\bar{\omega}_{*a} (1 - 3\eta_a/2) (\sigma_a \psi_{1a} \bar{\kappa}_1 - \varepsilon_a \psi_{3a} \bar{\kappa}_3 - \varepsilon_a \psi_{5a} \bar{\kappa}_5) \right. \\ & \quad \left. + \bar{\omega}_{*a} \eta_a (\sigma_a \psi_{2a} \bar{\kappa}_1 - \varepsilon_a \psi_{4a} \bar{\kappa}_3 - \varepsilon_a \psi_{6a} \bar{\kappa}_5) - \sigma_a \psi_{1a} \bar{\kappa}_2 + \varepsilon_a \psi_{3a} \bar{\kappa}_4 + \varepsilon_a \psi_{5a} \bar{\kappa}_6 \right]. \end{aligned} \quad (3.13)$$

To simplify the problem further, we can take moments of (3.13) and obtain a closed linear system for $\bar{\kappa}_n$. We first write (3.12) as

$$\bar{\kappa}_m = \sum_{n,b} c_{mn}^{(b)} \kappa_{nb}. \quad (3.14)$$

Now taking moments of (3.13), and summing over species, using (3.14), we obtain

$$\begin{aligned} & \frac{\Lambda}{\omega_*} \left(\bar{\kappa}_m + \sum_{a,n} \left\{ -\mathcal{T}_{mn}^{(a)} \chi_{1n}^{(a)} \bar{\kappa}_1 + \mathcal{E}_{mn}^{(a)} (\chi_{3n}^{(a)} \bar{\kappa}_3 + \chi_{5n}^{(a)} \bar{\kappa}_5) \right\} \right) \\ &= \sum_{a,n} \frac{i}{2} \left\{ \bar{\omega}_{*a} (1 - 3\eta_a/2) \left[\mathcal{T}_{mn}^{(a)} \chi_{1n}^{(a)} \bar{\kappa}_1 - \mathcal{E}_{mn}^{(a)} (\chi_{3n}^{(a)} \bar{\kappa}_3 + \chi_{5n}^{(a)} \bar{\kappa}_5) \right] \right. \\ & \quad + \bar{\omega}_{*a} \eta_a \left[\mathcal{T}_{mn}^{(a)} \chi_{2n}^{(a)} \bar{\kappa}_1 - \mathcal{E}_{mn}^{(a)} (\chi_{4n}^{(a)} \bar{\kappa}_3 + \chi_{6n}^{(a)} \bar{\kappa}_5) \right] \\ & \quad \left. - \mathcal{T}_{mn}^{(a)} \chi_{1n}^{(a)} \bar{\kappa}_2 + \mathcal{E}_{mn}^{(a)} (\chi_{3n}^{(a)} \bar{\kappa}_4 + \chi_{5n}^{(a)} \bar{\kappa}_6) \right\}, \end{aligned} \tag{3.15}$$

where we define the dimensionless quantities (see also Appendix C)

$$\mathcal{T}_{mn}^{(a)} = \frac{c_{mn}^{(a)} \sigma_a}{n_a T_a}, \tag{3.16}$$

$$\mathcal{E}_{mn}^{(a)} = \frac{c_{mn}^{(a)} \varepsilon_a}{n_a T_a}, \tag{3.17}$$

$$\chi_{mn}^{(a)} = \frac{1}{n_a} \int d^3 v F_{a0} \psi_{ma} \psi_{na}. \tag{3.18}$$

Equation (3.15) is the central result of this paper, a six-dimensional algebraic system of equations for unknowns $\bar{\kappa}_i$. As the system is homogeneous in these quantities, a non-trivial solution only exists if the determinant (of the matrix of coefficients) vanishes. This condition determines the eigenvalues Λ , which, according to (3.2)–(3.3), realise optimal growth of gyrokinetic free energy; see also the discussion in the following section.

Note that a solution of this system, i.e. Λ and $\{\bar{\kappa}_1, \dots, \bar{\kappa}_6\}$, can be substituted into the kinetic expression (3.13) to obtain the complete solution for the distribution functions g_a . When the spatial dependence of the solution is taken as $\delta(\ell - \ell_0)$, we obtain a set of orthogonal modes, which can be completed by introducing the null space of (3.13), namely all distribution functions satisfying $\bar{\kappa}_n = 0$ for all n (including but not limited to those satisfying $\kappa_{na} = 0$ for all a and n).

There are some properties of this system that help make solving it easier. First, there is the time reversal symmetry of collisionless gyrokinetics. That is, for any solution $\{\Lambda, \bar{\kappa}_1, \dots, \bar{\kappa}_6\}$, there is another solution $\{-\Lambda, \bar{\kappa}_1^*, \dots, \bar{\kappa}_6^*\}$, as can be seen by taking the complex conjugate of (3.15), and noting that Λ must be real by Hermiticity of (3.5). Thus, there are at most three unique non-zero values of Λ^2 to find.

In addition, due to the structure of X_{mn} (see Appendix C), the linear algebra can be decoupled into a single two-dimensional problem for $\bar{\kappa}_3$ and $\bar{\kappa}_4$, corresponding to perturbations of finite δA_{\parallel} , and a four-dimensional problem involving the remaining degrees of freedom, corresponding to mixed perturbations in $\delta\phi$ and δB_{\parallel} . We denote the positive eigenvalue of the former problem as Λ_3 , and those of the latter problem as Λ_1 and Λ_2 , reserving Λ_1 for the electrostatic root (when it is possible to identify one as such). For symmetry we denote the negative values as $\Lambda_{-n} = -\Lambda_n$.

3.2. Decomposition of energy balance

Now that we have shown how to calculate the optimal modes, we can show explicitly how they can be used to put the energy balance equation into a pleasing form. Generalising the

analysis of the schematic system, given by (1.1), we write the collisionless energy balance equation (2.1) as

$$\frac{d}{dt} \sum_{a,b} \left\langle T_a \int d^3 v \frac{g_a^*}{F_{a0}} \mathcal{H}_{ab} g_b \right\rangle = 2 \sum_{a,b} \left\langle T_a \int d^3 v \frac{g_a^*}{F_{a0}} \mathcal{D}_{ab} g_b \right\rangle \quad (3.19)$$

or, equivalently, using inner-product notation,

$$\frac{d}{dt} (\mathbf{g}, \mathcal{H}\mathbf{g}) = 2(\mathbf{g}, \mathcal{D}\mathbf{g}). \quad (3.20)$$

Now using completeness of the eigenmodes we can expand the state as

$$\mathbf{g} = \sum_n c_n(\ell) \mathbf{g}_n, \quad (3.21)$$

noting that there are only six eigenmodes of non-zero eigenvalues so the rest of the (infinite) solution space is the null space, i.e. $\Lambda_n = 0$ for $|n| \geq 4$. Now taking (3.5), we use orthogonality of eigenmodes of this (generalised) eigenproblem, i.e. $(\mathbf{g}_m, \mathcal{H}\mathbf{g}_n) = 0$ for $m \neq n$ unless $\Lambda_n = \Lambda_m$, and obtain

$$\sum_n \frac{d}{dt} \langle |c_n|^2 \rangle = \sum_n 2\Lambda_n \langle |c_n|^2 \rangle, \quad (3.22)$$

where we have normalised the eigenmodes such that $(\mathbf{g}_n, \mathcal{H}\mathbf{g}_n) = 1$. Note that (3.22), analogously to (1.3), demonstrates that the optimal modes, which are local extrema of D by virtue of being derived from a variational principle, also provide global extrema. That is, defining $\Lambda_{\max} = \max_n \Lambda_n$, we can conclude that

$$-2\Lambda_{\max} \leq \frac{d \ln H}{dt} \leq 2\Lambda_{\max}, \quad (3.23)$$

with equality (right-hand side and left-hand side) satisfied for the two eigenstates with $\Lambda = \pm \Lambda_{\max}$ (respectively). As noted in Helander & Plunk (2022), all these equations may be summed over k to yield linear and nonlinear bounds on the total free energy of the plasma fluctuations. In particular, (3.22), summed over wavenumbers, proves the necessity of instantaneous optimals, solutions with $\Lambda_n > 0$, for the existence of subcritical gyrokinetic turbulence, as noted already by Landreman *et al.* (2015).

It is worth emphasising, though it may be regarded as a trivial consequence of the total free energy balance, that a gyrokinetic plasma cannot sustain turbulence (subcritical or otherwise) without plasma gradients, since $\Lambda_n = 0$ and $\sum_k dH/dt \leq 0$ is nonlinearly true in that case.

4. Asymptotic limits

The general solution of (3.15), though easy to obtain numerically, is too lengthy and complicated to gain much insight from when written down in closed form. We therefore focus on a number of compact asymptotic results for the case of a hydrogen plasma, which also allow comparison with our previously published results (Helander & Plunk 2021, 2022).

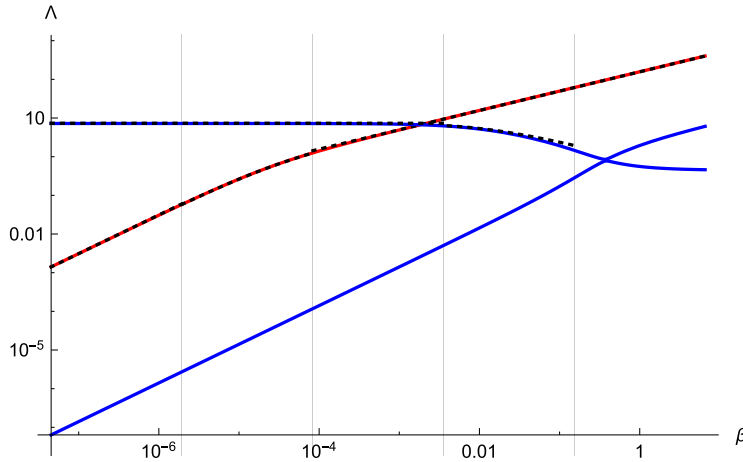


FIGURE 1. Summary of small wavenumber results. The numerical results for the mixed modes Λ_1 and Λ_2 are plotted in blue, while that for Λ_3 (the δA_{\parallel} mode) is given in red. Ranges of β (orders of ϵ ranging from 0 to 4), are separated visually by vertical grey lines at intermediate values ($\epsilon^{1/2}$, $\epsilon^{3/2}$, etc.). The asymptotic results are plotted in dashed black. Note that the growth rates are normalised to $|\omega_{i*}|$.

We order all parameters in terms of the small quantity

$$\epsilon = \sqrt{\frac{b_e}{b_i}} = \sqrt{\frac{m_e T_e}{m_i T_i}} \ll 1. \tag{4.1}$$

We take three limits according to the size of the perpendicular wavenumber relative to the Larmor scales, and we also consider different strengths of the plasma betas, but using the same ordering for the different betas, $\beta_e \sim \beta_i$. All other dimensionless parameters are assumed to be of the order of 1, i.e. $\eta_i \sim \eta_e \sim \tau \sim 1$, where $\tau = T_i/T_e$ and we assume that $\omega_{*i} \sim \omega_{*e}$ though we need not order these frequencies in terms of ϵ as this merely translates into an ordering of Λ , which could be normalised by their amplitude. In all cases where we numerically evaluate the solutions, we take $\beta_i = \beta_e = \beta$, $\omega_{*i} = -\omega_{*e} = \omega_*$, $\eta_i = \eta_e = \tau = 1$ and $\epsilon = 0.023337$ (square root of the electron–proton mass ratio). Note that the value of the parameters b_i and b_e are set exactly to a power of the ordering parameter according to the particular limit being taken, e.g. $b_i = \epsilon$ for the case $b_i \sim \epsilon$ for the values computed in figure 1.

4.1. *Small wavenumber limit: $b_i \sim \epsilon$ and $b_e \sim \epsilon^3$*

In this limit we must be careful to retain first-order contributions in the Bessel function expansions because the problem is singular if $b_e = b_i = 0$ is taken identically (H is not positive-definite in this case).

For Λ_1 and Λ_2 , we consider a number of limits on β . In the electrostatic limit ($\beta \sim \epsilon^2$) we have

$$\Lambda_1^2 = \frac{\tau \left(3(\tau + 1)\eta_e^2 \omega_{*e}^2 + 2(\omega_{*e} - \omega_{*i})^2 + 3\left(\frac{1}{\tau} + 1\right)\eta_i^2 \omega_{*i}^2 \right)}{8(\tau + 1)b_i}. \tag{4.2}$$

Note that this result is formally $\mathcal{O}(\epsilon^{-1})$ and $\Lambda_2 = 0$ at this order. One can compare this with (6.4) in Helander & Plunk (2022), the optimal adiabatic electron result, which has

qualitatively different behaviour, going to zero with η_i and also tending to zero with k_α . This is explained by the fact that the adiabatic electron limit is not obtained as a simple asymptotic limit of the general two-species result, because the ordering and solving of the electron gyrokinetic equation itself is necessary to obtain the adiabatic electron response. Thus, the two-species result here is not to be taken simply as a more complete result compared with the adiabatic electron result.

Allowing slightly large beta, $\beta \sim \epsilon^1$, the electromagnetic (δB_\parallel) effects start to mix, making Λ_1 no longer purely electrostatic:

$$\Lambda_1^2 = \frac{\tau \left(3(\tau + 1)\eta_e^2\omega_{*e}^2 + 2(\omega_{*e} - \omega_{*i})^2 + 3\left(\frac{1}{\tau} + 1\right)\eta_i^2\omega_{*i}^2 \right)}{4(\tau + 1)(2b_i + \tau\beta_e + 2\sqrt{\tau\beta_e\beta_i} + \beta_i)}. \tag{4.3}$$

Note that this expression encompasses the $\beta \sim \epsilon^2$ result (4.2). Note also, that the result can be interpreted as an (initial) finite- β stabilisation of the electrostatic result; see figure 1.

For the weakly electromagnetic mode, a single result encompasses all limits of β ($\beta_a \sim \epsilon^4$, $\beta_a \sim \epsilon^3$ and $\beta_a \sim \epsilon^2$ and larger):

$$\Lambda_3^2 = \frac{5\beta_e^2\eta_e^2\omega_{*e}^2}{16b_e(2b_e + \beta_e)}, \tag{4.4}$$

where we note that this result also applies to $b_i \sim 1$, as the electron contribution dominates. The result may be compared with our previous bound, i.e. the second term in (5.6) of Helander & Plunk (2022), which can be interpreted as a bound on the electromagnetic contribution to free energy growth. For general η_e one can verify that Λ_3 of (4.4) is always less than 1/4 of our previous bound, and goes to zero for $\eta_e = 0$, while our previous bound does not.

A critical value of β (of order ϵ^2) can be identified in this (small- b) limit, corresponding to the value of β above which the root Λ_3 exceeds the electrostatic root Λ_1 . An expression for this critical value can be obtained by setting $\Lambda_3 = \Lambda_1$ using (4.2) and (4.4), noting that the factor $2b_e$ can be neglected in the denominator, yielding

$$\beta_{e,crit} = \frac{2\tau b_e \left(3(\tau + 1)\eta_e^2\omega_{*e}^2 + 2(\omega_{*e} - \omega_{*i})^2 + 3\left(\frac{1}{\tau} + 1\right)\eta_i^2\omega_{*i}^2 \right)}{5(\tau + 1)b_i\eta_e^2\omega_{*e}^2}. \tag{4.5}$$

Curiously, we numerically observe that Λ_3 always seems to be at least as big as the magnetic root Λ_2 (associated with inclusion of δB_\parallel), so that the above critical β is the one of most relevance for overall stability, and simple asymptotic results such as the limits derived here may always be adequate to characterise the actual maximum growth rate of free energy. Note that the apparent divergence of $\beta_{e,crit}$ in the limit $\eta_e \rightarrow 0$, should be no cause for alarm, as we have assumed the ordering $\eta_e \sim 1$, in which the dominant contribution to Λ_3 is proportional to η_e . The result for Λ_3 obtained assuming $\eta_e = 0$, while being two orders smaller in ϵ , would of course be non-zero and result in a finite value of $\beta_{e,crit}$.

To summarise the features of this limit, and confirm the asymptotic results, we numerically solve for roots Λ_1 , Λ_2 and Λ_3 and compare them with the values computed from the asymptotic results listed above. Figure 1 shows the result.

4.2. Intermediate wavenumber limit: $b_i \sim \epsilon^{-1}$, $b_e \sim \epsilon$

First, we note that for all β ($\beta \sim \epsilon^2$, $\beta \sim \epsilon^1$, and $\beta \sim 1$ and larger), the expression given by (4.4) for Λ_3 still applies in this limit: the ion contribution is still subdominant, and $b_e \ll 1$ also applies here.

For the electrostatic limit ($\beta \sim \epsilon$), we obtain

$$\Lambda_1^2 = \frac{3\tau^2\eta_e^2\omega_{*e}^2}{8(\tau+1)} + \frac{\tau(\omega_{*e}^2(6(\tau+1)\eta_e^2+4) + 4(\eta_i-2)\omega_{*e}\omega_{*i} + (5\eta_i^2-4\eta_i+4)\omega_{*i}^2)}{16\sqrt{2\pi}(\tau+1)\sqrt{b_i}}, \quad (4.6)$$

which can be compared with our adiabatic-electron electrostatic bound, given by (6.4) of Helander & Plunk (2022). Note that we need to retain the second term, formally smaller than the first by a factor $\epsilon^{1/2}$, for this comparison. The results can be made comparable by setting $\omega_{*e} = 0$ and additionally taking $\omega_{*i} \rightarrow 0$ while holding $\eta_i\omega_{*i} \sim 1$; see the discussion following (4.2).

For $\beta \sim 1$ we obtain (at dominant order) the result

$$\Lambda_{1,2}^2 = \frac{\eta_e^2\omega_{*e}^2(P \pm \sqrt{P^2 - R})}{16(\tau+1)((\tau+2)\beta_e+2)}, \quad (4.7)$$

with

$$\left. \begin{aligned} P &= (9\tau^2 + 23\tau + 14)\beta_e^2 - (9\tau + 10)\tau\beta_e + 6\tau^2, \\ R &= 18\tau^2(\tau+1)\beta_e^2((\tau+2)\beta_e+2). \end{aligned} \right\} \quad (4.8)$$

Note that the dominant (first) term of (4.6) can be recovered as $\beta_e \rightarrow 0$, and that there is also an initial stabilisation, as compared with the electrostatic limit associated with finite β_e , as can be seen in figure 2.

We compute the critical β as before by equating the asymptotic forms of Λ_1 and Λ_3 for the regime where they intersect, $\beta \sim \epsilon^1$ (retaining the first term of (4.6) and the full form of (4.4)):

$$\beta_{e,\text{crit}} = \frac{\tau b_e(\sqrt{9\tau^2 + 60(\tau+1)} + 3\tau)}{5(\tau+1)}, \quad (4.9)$$

where we have selected the positive root to that equation. Figure 2 summarises the behaviour of the roots across the beta regimes, and confirms the asymptotic results.

4.3. Large wavenumber limit: $b_e \sim \epsilon^{-1}$, $b_i \sim \epsilon^{-3}$

For large b_e we obtain finally an asymptotic result for Λ_3 distinct from the previous result. For $\beta \sim \epsilon^{-1}$ or smaller, we obtain

$$\Lambda_3^2 = \frac{\beta_e^2\eta_e^2\omega_{*e}^2}{16\pi b_e^3}, \quad (4.10)$$

while for $\beta \sim \epsilon^{-2}$ we have

$$\Lambda_3^2 = \frac{\beta_e\eta_e^2\omega_{*e}^2}{4\sqrt{2\pi}b_e^{3/2}}. \quad (4.11)$$

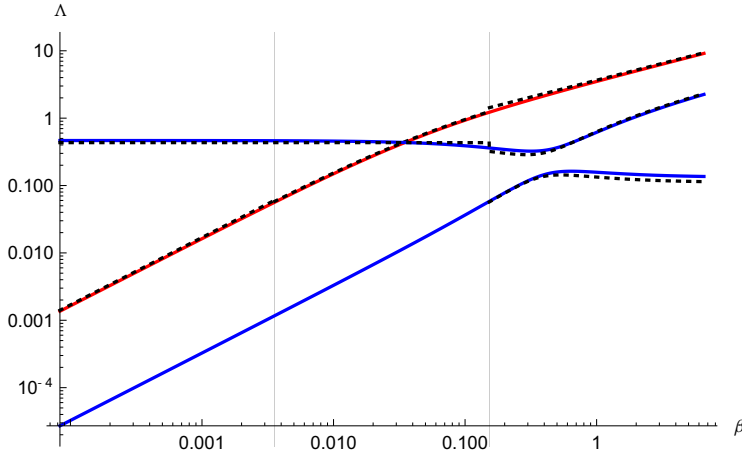


FIGURE 2. Summary of medium wavenumber results. The numerical results for the mixed modes Λ_1 and Λ_2 are plotted in blue, while that for Λ_3 (the δA_{\parallel} mode) is given in red. Ranges of β (orders of ϵ ranging from 0 to 2), are separated visually by vertical grey lines at intermediate values ($\epsilon^{1/2}$, $\epsilon^{3/2}$, etc.). The asymptotic results are plotted in dashed black. Note that the growth rates are normalised to $|\omega_{i*}|$.

An electrostatic root is obtained for $\beta \sim 1$, and also survives for $\beta \sim \epsilon^{-1}$:³

$$\Lambda_1^2 = \frac{\tau^2 \eta_e^2 \omega_{*e}^2}{8\pi(\tau + 1)^2 b_e}. \tag{4.12}$$

Note we do not retain higher-order contributions for comparison with the adiabatic electron result, which does not discriminate between regimes of b_e , since that comparison was already made for the intermediate limit $b_i \sim \epsilon^{-1}$.

For $\beta \sim \epsilon^{-1}$, we find an additional electromagnetic root appears, which, curiously, matches the other electromagnetic root Λ_3 in this limit

$$\Lambda_2^2 = \frac{\beta_e^2 \eta_e^2 \omega_{*e}^2}{16\pi b_e^3}. \tag{4.13}$$

For $\beta \sim \epsilon^{-2}$, the roots continue to match:

$$\Lambda_2^2 = \frac{\beta_e \eta_e^2 \omega_{*e}^2}{4\sqrt{2\pi} b_e^{3/2}}. \tag{4.14}$$

The critical value of β above which the magnetic roots exceed the electrostatic one is derived as before from the results for $\beta \sim \epsilon^{-1}$:

$$\beta_{e,\text{crit}} = \frac{\sqrt{2}\tau b_e}{\tau + 1}. \tag{4.15}$$

The results of this limit are summarised in [figure 3](#).

³As seen in [figure 3](#), it also seems to be valid for $\beta \sim \epsilon^{-2}$ but we did not prove this.

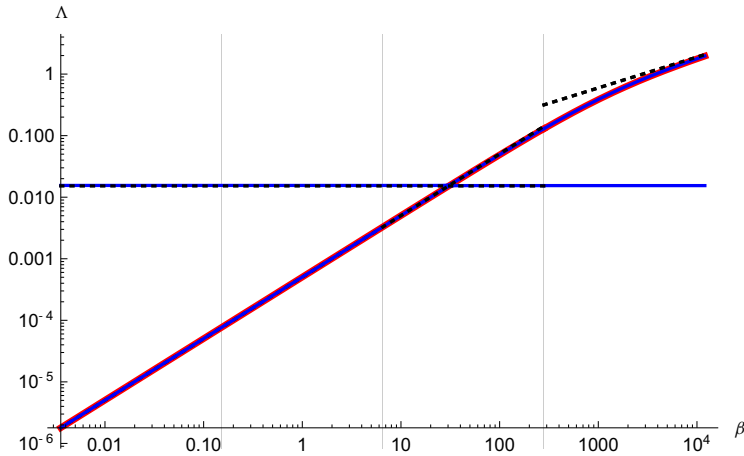


FIGURE 3. Summary of large wavenumber results. The numerical results for the mixed modes Λ_1 and Λ_2 are plotted in blue, while that for Λ_3 (the δA_{\parallel} mode) is given in red. Ranges of β (orders of ϵ ranging from 1 to -1), are separated visually by vertical grey lines at intermediate values ($\epsilon^{1/2}$, $\epsilon^{3/2}$, etc.). The asymptotic results are plotted in dashed black. Note that the growth rates are normalised to $|\omega_{i*}|$. Note that, curiously, the red curve coincides with one branch of the blue curve, in each range of β .

5. Discussion

Although the essential ideas involved in calculating ‘optimal modes’ are simple, the algebra involved is sufficiently complex that a general closed-form solution is too lengthy to express in a useful way. Thus, we have provided a number of compact asymptotic results to demonstrate the essential behaviour.

These results compare as expected with the bounds presented in Helander & Plunk (2021, 2022), i.e. they are always less than or equal to the previous bounds, and similar qualitatively, though in some special cases much smaller. The adiabatic electron result of Helander & Plunk (2022) is a curious case to compare. One might expect that the two-species electrostatic, long-wavelength limit obtained here might give a similar result, but this is not the case because the adiabatic electron response requires that the electron gyrokinetic equation be ordered and solved at the outset. Thus, the two-species result is not simply a generalisation of the one-species adiabatic case. On the one hand, the two-species calculation is able to treat closed-field-line geometries (dipole, Z-pinch), and obtain bounds on the MHD-interchange-like instability there, whose growth tends to a constant as $k_{\perp} \rightarrow 0$; see, for instance, Ricci *et al.* (2006). On the other hand, the adiabatic-electron result provides a lower bound, and compares well with expectations of the ITG mode, for which $\gamma \rightarrow 0$ as $k_{\perp} \rightarrow 0$ (Kadomtsev & Pogutse 1970; Biglari, Diamond & Rosenbluth 1989). This demonstrates that it is possible to improve and reduce the complexity of the optimal mode analysis by first applying limits to the fully gyrokinetic system, as should be useful, e.g., for the case of trapped electron modes where a bounce-averaged electron response can be used.

We have mentioned the possible application of optimal modes to the study of subcritical turbulence, in which case normal mode analysis predicts linear stability. As a most basic result, one can conclude that a gyrokinetic system can only sustain turbulence in the presence of background gradients, otherwise $\omega_{*a} = 0$ and $\Lambda_n = 0$, implying that $\sum_k dH/dt \leq 0$, including collisions. The steady state of such a system can only be a

state of zero fluctuations. Though transient growth in such systems may be observed in other norms than the free energy (Camporeale, Burgess & Passot 2009; Podesta 2010), such growth cannot, via the gyrokinetic nonlinearity, support sustained turbulence. In the case where some plasma gradient is present, but normal linear analysis predicts stability, the growth of free energy for fixed k is bounded by the optimal rates. For example, the electrostatic result (e.g. Λ_1 of (4.2)) bounds the observable growth both linearly and nonlinearly for subcritical turbulence driven by the universal instability, i.e. Λ_1 yields an explicit calculation of the measure proposed by Landreman *et al.* (2015). Turbulence driven by the parallel velocity gradient (Barnes *et al.* 2011) would be another potential application of optimal mode analysis; the equilibrium parallel velocity gradient is neglected in the present analysis, but would be straightforward to include.

We have assumed non-zero δB_{\parallel} in our analysis, which is chiefly to blame for the added complexity of the algebra, making the results quite general for (local flux-tube) gyrokinetics. We note that its effect seems mostly subdominant to that of δA_{\parallel} in the sense that at sufficiently low β the electrostatic result is dominant, while at large β , a decoupled mode associated with fluctuations in δA_{\parallel} is dominant, so that the overall maximum growth ($\max_n \Lambda_n$) is never strongly affected by the inclusion of δB_{\parallel} . Thus, the weakly electromagnetic result, in which we assume $\delta B_{\parallel} \approx 0$, may be sufficient to treat many cases of interest, at least if the main goal is establishing overall bounds.

An apparent limitation of our results comes from the lack of information retained of the geometry of the magnetic field. The only place the metrics appear in our results is in the quantity $k_{\perp} = |k_{\psi} \nabla \psi + k_{\alpha} \nabla \alpha|$. However, there is an important physical mechanism that remains here, though somewhat obscured by the use of magnetic coordinates, namely the compression of flux surfaces. This is determined by the metric $|\nabla \psi|$, which directly affects the size of the plasma gradients, as measured in conventional (non-magnetic) spatial coordinates, e.g. ∇T_a (Angelino *et al.* 2009). The effect is revealed when considering a mode in two different magnetic configurations with a fixed value of k_{\perp} . Roughly speaking, the configuration with larger compression ($|\nabla \psi|$), must, given equal $B = |\nabla \psi \times \nabla \alpha|$, have larger k_{α} , at equal k_{\perp} , and therefore a greater drive ω_{*a} and resulting optimal growth rates. In addition to being known in tokamaks, this effect has recently been found to be important within the configuration space of the W7-X experiment (Stroteich *et al.* 2022).

In Parts 1 and 2 in this series, we have focused on the Helmholtz free energy, but we note that this is not the only possible choice. As we have seen, the resulting picture of stability in this case only depends on the strength of certain non-conservative terms in the gyrokinetic equation and, aside from the effect just described, much is lost of the magnetic geometry. In particular, the mechanism of resonance does not play an explicit role, i.e. the parallel advection and magnetic drift terms, with the latter being known to explain differences in the stability properties of different kinds of magnetic confinement devices (stellarators, tokamaks, etc.). In Part 3 of this series, we will show how the lost effects of magnetic geometry can be recovered by use of a more general notion of free energy.

Acknowledgements

Editor Alex Schekochihin thanks the referees for their advice in evaluating this article.

Funding

This work has been carried out within the framework of the EUROfusion Consortium, funded by the European Union via the Euratom Research and Training Programme (Grant Agreement No.101052200 – EUROfusion). Views and opinions expressed are however those of the author(s) only and do not necessarily reflect those of the European Union or

the European Commission. Neither the European Union nor the European Commission can be held responsible for them. This work was partly supported by a grant from the Simons Foundation (560651, PH).

Declaration of interests

The authors report no conflict of interest.

Appendix A. \mathcal{H} and \mathcal{D}

Taking (2.2) and (2.3) and using the field equations, we obtain

$$\begin{aligned}
 D = & \sum_{a,b} \frac{i\omega_{*a}}{2n_a n_b} \left\langle \int d^3 v \int d^3 v' g_a^*(v) g_b(v') \right. \\
 & \times \left[\left(1 - \frac{3\eta_a}{2} \right) (\sigma_a \sigma_b \psi_{1a} \psi'_{1b} - \varepsilon_a \varepsilon_b \psi_{3a} \psi'_{3b} - \varepsilon_a \varepsilon_b \psi_{5a} \psi'_{5b}) \right. \\
 & \left. \left. + \eta_a (\sigma_a \sigma_b \psi_{2a} \psi'_{1b} - \varepsilon_a \varepsilon_b \psi_{4a} \psi'_{3b} - \varepsilon_a \varepsilon_b \psi_{6a} \psi'_{5b}) \right] \right\rangle + \text{c.c.}, \tag{A1}
 \end{aligned}$$

and

$$\begin{aligned}
 H = & \sum_a \left\langle \int d^3 v \frac{T_a |g_a|^2}{F_{a0}} \right\rangle - \sum_a \frac{1}{n_a T_a} \left\langle \left| \sum_b \frac{1}{n_b} \int d^3 v \sigma_a \sigma_b \psi_{1b} g_b \right|^2 \right\rangle \\
 & + \sum_{a,b} \frac{\varepsilon_a \varepsilon_b}{n_a n_b} \left\langle \int d^3 v \int d^3 v' g_a^*(v) g_b(v') [\psi_{3a} \psi'_{3b} + \psi_{5a} \psi'_{5b}] \right\rangle + \text{c.c.} \tag{A2}
 \end{aligned}$$

We define the variation of an arbitrary functional F with respect to the distribution function g_a as

$$\frac{\delta F}{\delta g_a} = \lim_{\epsilon \rightarrow 0} \frac{d}{d\epsilon} F[g_a + \epsilon h], \tag{A3}$$

where h is an arbitrary function of phase space variables. Equations (A1) and (A2) yield

$$\frac{\delta D}{\delta g_a} = \left\langle \int d^3 v \frac{T_a}{F_{a0}} h^* \left\{ \sum_b \mathcal{D}_{ab} g_b \right\} \right\rangle + \text{c.c.}, \tag{A4}$$

and

$$\frac{\delta H}{\delta g_a} = \left\langle \int d^3 v \frac{T_a}{F_{a0}} h^* \left\{ \sum_b \mathcal{H}_{ab} g_b \right\} \right\rangle + \text{c.c.}, \tag{A5}$$

where the operators \mathcal{D} and \mathcal{H} are as defined in (3.6) and (3.7). Note that we have exchanged species labels, and dummy velocity variables of integration to obtain this form. Because h is arbitrary, these forms substituted into (3.4) yield (3.5).

Appendix B. Bessel-type integrals

To calculate the various integrals involving Bessel functions, we begin with a general form of Weber’s integral:

$$\begin{aligned} \mathcal{I}_\nu(p, a_1, a_2) &= \int_0^\infty \exp(-pt^2) J_\nu(a_1 t) J_\nu(a_2 t) t \, dt \\ &= \frac{1}{2p} \exp\left(\frac{-a_1^2 - a_2^2}{4p}\right) I_\nu\left(\frac{a_1 a_2}{2p}\right) \end{aligned} \tag{B1}$$

where I_ν is the modified Bessel function of order ν . The integrals we need to evaluate can be conveniently found in terms of \mathcal{I}_ν . We define

$$G_{\perp m}(b) = 2 \int_0^\infty x_\perp^{m+1} \exp(-x_\perp^2) J_0^2(\sqrt{2b}x_\perp) \, dx_\perp, \tag{B2a}$$

$$G_{\perp m}^{(1)}(b) = 2 \int_0^\infty x_\perp^{m+2} \exp(-x_\perp^2) J_0(\sqrt{2b}x_\perp) J_1(\sqrt{2b}x_\perp) \, dx_\perp, \tag{B2b}$$

$$G_{\perp m}^{(2)}(b) = 2 \int_0^\infty x_\perp^{m+3} \exp(-x_\perp^2) J_1^2(\sqrt{2b}x_\perp) \, dx_\perp, \tag{B2c}$$

where m is assumed to be even. Now we note that these integrals can be evaluated in terms of Weber’s integral:

$$G_{\perp m}(b) = 2 \left[\left(-\frac{d}{dp}\right)^{m/2} \mathcal{I}_0(p, \sqrt{2b}, \sqrt{2b}) \right]_{p=1}, \tag{B3a}$$

$$G_{\perp m}^{(1)}(b) = 2 \left[\left(-\frac{d}{dp}\right)^{m/2} \left(-\frac{d}{d\lambda}\right) \mathcal{I}_0(p, \lambda, \sqrt{2b}) \right]_{p=1, \lambda=\sqrt{2b}}, \tag{B3b}$$

$$G_{\perp m}^{(2)}(b) = 2 \left[\left(-\frac{d}{dp}\right)^{m/2} \left(-\frac{d}{d\lambda_1}\right) \left(-\frac{d}{d\lambda_2}\right) \mathcal{I}_0(p, \lambda_1, \lambda_2) \right]_{p=1, \lambda_1=\lambda_2=\sqrt{2b}}. \tag{B3c}$$

The above relations allows us to evaluate the functions

$$G_{m,n}(b) = G_{\perp m}(b) G_{\parallel n}, \tag{B4a}$$

$$G_{m,n}^{(1)}(b) = G_{\perp m}^{(1)}(b) G_{\parallel n}, \tag{B4b}$$

$$G_{m,n}^{(2)}(b) = G_{\perp m}^{(2)}(b) G_{\parallel n}, \tag{B4c}$$

where

$$G_{\parallel n} = \frac{1}{\sqrt{\pi}} \int_{-\infty}^\infty \exp -x_\parallel^2 x_\parallel^n \, dx_\parallel = \frac{1 + (-1)^n}{2\sqrt{\pi}} \Gamma_E\left(\frac{1+n}{2}\right), \tag{B5}$$

and Γ_E is the Euler gamma function.

Appendix C. $\mathbf{X}(b)$

Bessel functions of various orders enter into the symmetric matrix \mathbf{X} , written as a function of b , depending on the species, whose elements are

$$X_{mn}(b_a) = \frac{1}{n_{0a}} \int d^3 v F_{a0} \psi_{ma} \psi_{na}, \quad (\text{C1})$$

where ψ_{ma} is the m th dimensionless velocity function that appears in the various moments that enter the free energy drive term D . Account for symmetry and oddness over v_{\parallel} integration, \mathbf{X} has the following form:

$$\mathbf{X}(b) = \begin{pmatrix} X_{11}(b) & X_{12}(b) & 0 & 0 & X_{15}(b) & X_{16}(b) \\ X_{12}(b) & X_{22}(b) & 0 & 0 & X_{25}(b) & X_{26}(b) \\ 0 & 0 & X_{33}(b) & X_{34}(b) & 0 & 0 \\ 0 & 0 & X_{34}(b) & X_{44}(b) & 0 & 0 \\ X_{15}(b) & X_{25}(b) & 0 & 0 & X_{55}(b) & X_{56}(b) \\ X_{16}(b) & X_{26}(b) & 0 & 0 & X_{56}(b) & X_{66}(b) \end{pmatrix}. \quad (\text{C2})$$

The elements X_{mn} are evaluated using the functions $G_{m,n}(b)$, $G_{m,n}^{(2)}(b)$ and $G_{m,n}^{(1)}(b)$, defined in the previous section. Following convention, we then evaluate them in terms of the usual gyrokinetic gamma functions

$$\Gamma_n(b) = \exp(-b) I_n(b). \quad (\text{C3})$$

Thus, X_{mn} are, for b of arbitrary size, as follows:

$$X_{11}(b) = G_{0,0}(b) = \Gamma_0(b), \quad (\text{C4})$$

$$X_{12}(b) = G_{0,2}(b) + G_{2,0}(b) = \left(\frac{3}{2} - b\right) \Gamma_0(b) + b \Gamma_1(b), \quad (\text{C5})$$

$$X_{15}(b) = G_{0,0}^{(1)}(b) = \sqrt{\frac{b}{2}} (\Gamma_0(b) - \Gamma_1(b)), \quad (\text{C6})$$

$$X_{16}(b) = G_{0,2}^{(1)}(b) + G_{2,0}^{(1)}(b) = -\frac{\sqrt{b} ((3b - 5)\Gamma_0(b) + (5 - 4b)\Gamma_1(b) + b\Gamma_2(b))}{2\sqrt{2}}, \quad (\text{C7})$$

$$\begin{aligned} X_{22}(b) &= G_{0,4}(b) + 2G_{2,2}(b) + G_{4,0}(b) \\ &= \frac{1}{4} ((6b^2 - 20b + 15) \Gamma_0(b) + 2b ((10 - 4b)\Gamma_1(b) + b\Gamma_2(b))), \end{aligned} \quad (\text{C8})$$

$$X_{25}(b) = G_{0,2}^{(1)}(b) + G_{2,0}^{(1)}(b) = -\frac{\sqrt{b} ((3b - 5)\Gamma_0(b) + (5 - 4b)\Gamma_1(b) + b\Gamma_2(b))}{2\sqrt{2}}, \quad (\text{C9})$$

$$\begin{aligned} X_{26}(b) &= G_{0,4}^{(1)}(b) + 2G_{2,2}^{(1)}(b) + G_{4,0}^{(1)}(b) \\ &= \frac{\sqrt{b}}{4\sqrt{2}} ((10b^2 - 42b + 35) \Gamma_0(b) + (-15b^2 + 56b - 35) \Gamma_1(b)) \\ &\quad + \frac{b^{3/2}}{4\sqrt{2}} (2(3b - 7)\Gamma_2(b) - b\Gamma_3(b)), \end{aligned} \quad (\text{C10})$$

$$X_{33}(b) = G_{0,2}(b) = \frac{\Gamma_0(b)}{2}, \tag{C11}$$

$$X_{34}(b) = G_{0,4}(b) + G_{2,2}(b) = \frac{1}{4} ((5 - 2b)\Gamma_0(b) + 2b\Gamma_1(b)), \tag{C12}$$

$$\begin{aligned} X_{44}(b) &= G_{0,6}(b) + 2G_{2,4}(b) + G_{4,2}(b) \\ &= \frac{1}{8} ((6b^2 - 28b + 35)\Gamma_0(b) + 2b((14 - 4b)\Gamma_1(b) + b\Gamma_2(b))), \end{aligned} \tag{C13}$$

$$X_{55}(b) = G_{0,0}^{(2)}(b) = \frac{1}{4} (3b\Gamma_0(b) + (2 - 4b)\Gamma_1(b) + b\Gamma_2(b)), \tag{C14}$$

$$\begin{aligned} X_{56}(b) &= G_{0,2}^{(2)}(b) + G_{2,0}^{(2)}(b) \\ &= \frac{1}{8} ((15b^2 - 32b + 10)\Gamma_1(b) + (23 - 10b)b\Gamma_0(b) \\ &\quad + b((9 - 6b)\Gamma_2(b) + b\Gamma_3(b))), \end{aligned} \tag{C15}$$

$$\begin{aligned} X_{66}(b) &= G_{0,4}^{(2)}(b) + 2G_{2,2}^{(2)}(b) + G_{4,0}^{(2)}(b) \\ &= \frac{1}{16} (b(35b^2 - 188b + 217)\Gamma_0(b) + (-56b^3 + 284b^2 - 308b + 70)\Gamma_1(b)) \\ &\quad + \frac{b}{16} ((28b^2 - 116b + 91)\Gamma_2(b) + b((20 - 8b)\Gamma_3(b) + b\Gamma_4(b))). \end{aligned} \tag{C16}$$

C.1. Asymptotic forms of X_{mn}

For small b we have, to first order, the following forms of X_{mn} :

$$\left. \begin{aligned} X_{11}(b) &\approx 1 - b, & X_{12}(b) &\approx \frac{3}{2} - \frac{5b}{2}, & X_{15}(b) &\approx \frac{\sqrt{b}}{\sqrt{2}}, & X_{16}(b) &\approx \frac{5\sqrt{b}}{2\sqrt{2}}, \\ X_{22}(b) &\approx \frac{15}{4} - \frac{35b}{4}, & X_{25}(b) &\approx \frac{5\sqrt{b}}{2\sqrt{2}}, & X_{26}(b) &\approx \frac{35\sqrt{b}}{4\sqrt{2}}, & X_{33}(b) &\approx \frac{1}{2} - \frac{b}{2}, \\ X_{34}(b) &\approx \frac{5}{4} - \frac{7b}{4}, & X_{44}(b) &\approx \frac{35}{8} - \frac{63b}{8}, & X_{55}(b) &\approx b, & X_{56}(b) &\approx \frac{7b}{2}, \\ & & X_{66}(b) &\approx \frac{63b}{4}. \end{aligned} \right\} \tag{C17}$$

For large b we use the following asymptotic forms of X_{mn} :

$$\left. \begin{aligned} X_{11}(b) &\approx \frac{1}{\sqrt{2\pi\sqrt{b}}}, & X_{12}(b) &\approx \frac{1}{\sqrt{2\pi\sqrt{b}}}, & X_{15}(b) &\approx \frac{1}{4\sqrt{\pi b}}, & X_{16}(b) &\approx \frac{1}{4\sqrt{\pi b}}, \\ X_{22}(b) &\approx \sqrt{\frac{2}{\pi b}}, & X_{25}(b) &\approx \frac{1}{4\sqrt{\pi b}}, & X_{26}(b) &\approx \frac{1}{2\sqrt{\pi b}}, & X_{33}(b) &\approx \frac{1}{2\sqrt{2\pi\sqrt{b}}}, \\ X_{34}(b) &\approx \frac{1}{\sqrt{2\pi\sqrt{b}}}, & X_{44}(b) &\approx \frac{3}{\sqrt{2\pi\sqrt{b}}}, & X_{55}(b) &\approx \frac{1}{2\sqrt{2\pi\sqrt{b}}}, & X_{56}(b) &\approx \frac{1}{\sqrt{2\pi\sqrt{b}}}, \\ & & X_{66}(b) &\approx \frac{3}{\sqrt{2\pi\sqrt{b}}}. \end{aligned} \right\} \tag{C18}$$

Appendix D. Exact results for the case of a hydrogen plasma

We give the exact result of optimal growth rates for the electrostatic and weakly electromagnetic cases, defining for compactness the species-dependent elements

$$X_{mn}^a = X_{mn}(b_a). \quad (D1)$$

D.1. Electrostatic limit

We have

$$\Lambda_1^2 = \frac{C_{ee}^{(1)}\omega_{*e}^2 + C_{ee}^{(1)}\omega_{*e}\omega_{*i} + C_{ii}^{(1)}\omega_{*i}^2}{16(\tau + 1)(\tau + 1 - \tau X_{11}^e - X_{11}^i)}, \quad (D2)$$

$$C_{ii}^{(1)} = \tau X_{11}^e \left((2 - 3\eta_i)^2 X_{11}^i + 4\eta_i \left((2 - 3\eta_i) X_{12}^i + \eta_i X_{22}^i \right) \right) - 4\eta_i^2 \left((X_{12}^i)^2 - X_{11}^i X_{22}^i \right), \quad (D3)$$

$$C_{ee}^{(1)} = \tau X_{11}^e \left((2 - 3\eta_e)^2 X_{11}^e + 4\tau \eta_e^2 X_{22}^e \right) + 4\tau \eta_e \left(X_{11}^e \left((2 - 3\eta_e) X_{12}^e + \eta_e X_{22}^e \right) - \tau \eta_e (X_{12}^e)^2 \right), \quad (D4)$$

$$C_{ie}^{(1)} = -2\tau \left((3\eta_e - 2) X_{11}^e - 2\eta_e X_{12}^e \right) \left((3\eta_i - 2) X_{11}^i - 2\eta_i X_{12}^i \right). \quad (D5)$$

D.2. Weakly electromagnetic ‘ δA_{\parallel} modes’

We have

$$\Lambda_3^2 = \frac{C_{ee}^{(3)}\omega_{*e}^2 + C_{ie}^{(3)}\omega_{*e}\omega_{*i} + C_{ii}^{(3)}\omega_{*i}^2}{16b_e b_i (b_i \beta_e X_{33}^e + b_e \beta_i X_{33}^i + b_e b_i)}, \quad (D6)$$

$$C_{ii}^{(3)} = b_e \beta_i \left(b_i \beta_e X_{33}^e \left((2 - 3\eta_i)^2 X_{33}^i + 4\eta_i \left((2 - 3\eta_i) X_{34}^i + \eta_i X_{44}^i \right) \right) - 4b_e^2 \beta_i^2 \eta_i^2 \left((X_{34}^i)^2 - X_{33}^i X_{44}^i \right) \right), \quad (D7)$$

$$C_{ee}^{(3)} = b_i \beta_e \left(X_{33}^e \left(4b_i \beta_e \eta_e^2 X_{44}^e + b_e (2 - 3\eta_e)^2 \beta_i X_{33}^i \right) + 4\eta_e b_i \beta_e \left((b_e \beta_i X_{33}^i \left((2 - 3\eta_e) X_{34}^e + \eta_e X_{44}^e \right) - b_i \beta_e \eta_e (X_{34}^e)^2 \right) \right), \quad (D8)$$

$$C_{ie}^{(3)} = -2b_e b_i \beta_e \beta_i \left((3\eta_e - 2) X_{33}^e - 2\eta_e X_{34}^e \right) \left((3\eta_i - 2) X_{33}^i - 2\eta_i X_{34}^i \right). \quad (D9)$$

REFERENCES

- ANGELINO, P., GARBET, X., VILLARD, L., BOTTINO, A., JOLLIET, S., GHENDRIH, PH., GRANDGIRARD, V., MCMILLAN, B.F., SARAZIN, Y., DIF-PRADALIER, G., *et al.* 2009 Role of plasma elongation on turbulent transport in magnetically confined plasmas. *Phys. Rev. Lett.* **102**, 195002.
- BARNES, M., PARRA, F.I., HIGHCOCK, E.G., SCHEKOCIHIN, A.A., COWLEY, S.C. & ROACH, C.M. 2011 Turbulent transport in tokamak plasmas with rotational shear. *Phys. Rev. Lett.* **106**, 175004.
- BIGLARI, H., DIAMOND, P.H. & ROSENBLUTH, M.N. 1989 Toroidal ion-pressure-gradient-driven drift instabilities and transport revisited. *Phys. Fluids B: Plasma Phys.* **1** (1), 109–118.
- BOURDELLE, C., CITRIN, J., BAIOCCHI, B., CASATI, A., COTTIER, P., GARBET, X. & IMBEAUX, F. 2015 Core turbulent transport in tokamak plasmas: bridging theory and experiment with QuaLiKiz. *Plasma Phys. Control. Fusion* **58** (1), 014036.

- CAMPOREALE, E., BURGESS, D. & PASSOT, T. 2009 Transient growth in stable collisionless plasma. *Phys. Plasmas* **16** (3), 030703.
- DELSOLE, T. 2004 The necessity of instantaneous optimals in stationary turbulence. *J. Atmos. Sci.* **61** (9), 1086–1091.
- FARRELL, B.F. & IOANNOU, P.J. 1996 Generalized stability theory. Part I: autonomous operators. *J. Atmos. Sci.* **53** (14), 2025–2040.
- HATCH, D.R., JENKO, F., BAÑÓN NAVARRO, A., BRATANOV, V., TERRY, P.W. & PUESCHEL, M.J. 2016 Linear signatures in nonlinear gyrokinetics: interpreting turbulence with pseudospectra. *New J. Phys.* **18** (7), 075018.
- HELANDER, P. & PLUNK, G.G. 2021 Upper bounds on gyrokinetic instabilities in magnetized plasmas. *Phys. Rev. Lett.* **127**, 155001.
- HELANDER, P. & PLUNK, G.G. 2022 Energetic bounds on gyrokinetic instabilities. Part 1. Fundamentals. *J. Plasma Phys.* **88** (2), 905880207.
- HORTON, W. 1999 Drift waves and transport. *Rev. Mod. Phys.* **71**, 735–778.
- KADOMTSEV, B.B. & POGUTSE, O.P. 1970 Turbulence in toroidal systems. *Rev. Plasmas Phys.* **5** (6), 249–400.
- LANDREMAN, M., PLUNK, G.G. & DORLAND, W. 2015 Generalized universal instability: transient linear amplification and subcritical turbulence. *J. Plasma Phys.* **81** (5), 905810501.
- PODESTA, J.J. 2010 Transient growth in stable linearized Vlasov–Maxwell plasmas. *Phys. Plasmas* **17** (12), 122101.
- RICCI, P., ROGERS, B.N., DORLAND, W. & BARNES, M. 2006 Gyrokinetic linear theory of the entropy mode in a Z pinch. *Phys. Plasmas* **13** (6), 062102.
- SHANKAR, R. 1994 *Principles of Quantum Mechanics*, 2nd ed. Plenum Press.
- STAEBLER, G.M., KINSEY, J.E. & WALTZ, R.E. 2007 A theory-based transport model with comprehensive physics. *Phys. Plasmas* **14** (5), 055909.
- STROTEICH, S., XANTHOPOULOS, P., PLUNK, G. & SCHNEIDER, R. 2022 Seeking turbulence optimized configurations for the Wendelstein 7-X stellarator. *J. Plasma Phys.* (submitted).